INTERFACE

rsif.royalsocietypublishing.org

Research

Cite this article: Mohammadi H, Arora PD, Simmons CA, Janmey PA, McCulloch CA. 2015 Inelastic behaviour of collagen networks in cell–matrix interactions and mechanosensation. *J. R. Soc. Interface* **12**: 20141074.
http://dx.doi.org/10.1098/rsif.2014.1074

Received: 25 September 2014
Accepted: 17 October 2014

Subject Areas:
biomaterials, biophysics, biomechanics

Keywords:
collagen gels, plasticity, remodelling, cell surface area

Author for correspondence:
Hamid Mohammadi
e-mail: hamid.mohammadi@utoronto.ca

Electronic supplementary material is available at http://dx.doi.org/10.1098/rsif.2014.1074 or via http://rsif.royalsocietypublishing.org.

THE ROYAL SOCIETY PUBLISHING

Inelastic behaviour of collagen networks in cell–matrix interactions and mechanosensation

Hamid Mohammadi[1], Pamma D. Arora[1], Craig A. Simmons[2], Paul A. Janmey[3] and Christopher A. McCulloch[1]

[1]Matrix Dynamics Group, and [2]Institute of Biomaterials and Biomedical Engineering, University of Toronto, Toronto, Ontario, Canada
[3]Institute for Medicine and Engineering, University of Pennsylvania, Philadelphia, PA, USA

The mechanical properties of extracellular matrix proteins strongly influence cell-induced tension in the matrix, which in turn influences cell function. Despite progress on the impact of elastic behaviour of matrix proteins on cell–matrix interactions, little is known about the influence of inelastic behaviour, especially at the large and slow deformations that characterize cell-induced matrix remodelling. We found that collagen matrices exhibit deformation rate-dependent behaviour, which leads to a transition from pronounced elastic behaviour at fast deformations to substantially inelastic behaviour at slow deformations (1 μm min^{-1}, similar to cell-mediated deformation). With slow deformations, the inelastic behaviour of floating gels was sensitive to collagen concentration, whereas attached gels exhibited similar inelastic behaviour independent of collagen concentration. The presence of an underlying rigid support had a similar effect on cell–matrix interactions: cell-induced deformation and remodelling were similar on 1 or 3 mg ml^{-1} attached collagen gels while deformations were two- to fourfold smaller in floating gels of high compared with low collagen concentration. In cross-linked collagen matrices, which did not exhibit inelastic behaviour, cells did not respond to the presence of the underlying rigid foundation. These data indicate that at the slow rates of collagen compaction generated by fibroblasts, the inelastic responses of collagen gels, which are influenced by collagen concentration and the presence of an underlying rigid foundation, are important determinants of cell–matrix interactions and mechanosensation.

1. Introduction

The markedly complex architecture, composition and mechanics of connective tissue matrices strongly influence cellular processes such as mechanosensation and metastatic invasion of extracellular matrices by malignant cells [1]. The ability of cells to sense the mechanical properties of matrix substrates is dependent on cell-generated forces, which enable cells to deform and sense the resistance of substrates [2,3]. Resistance to cell-induced deformation depends on the inherent stiffness of the substrate and is measured as various elastic moduli (e.g. shear, Young's), which apply to different types of deformation [4]. For example, linearly elastic substrates exhibit constant resistance to cell-induced deformation over a wide range of cell-generated forces [5]. By contrast, the resistance of nonlinear elastic substrates depends on the amplitude of cell-induced deformation, and some nonlinear elastic substrates such as cross-linked collagen gels exhibit strain stiffening when cell-induced deformation forces are increased [5]. The strain-dependent properties of both linear and nonlinear elastic substrates are reversible and are not associated with plastic deformation [6]. By comparison, substrates that exhibit internal inelastic properties (viscous and plastic) can deform continuously and permanently without rupture during the application of cell-generated forces [6]. Substrates that exhibit both elastic and inelastic behaviours are often elastic up to a critical deformation point [7]. Beyond this critical

point, the substrate will exhibit inelastic behaviour, and the proportional relationship between force and deformation no longer applies. For these types of substrates, inelastic behaviours need to be considered in the context of cellular mechanosensing and matrix invasion.

Polyacrylamide gels are well-established substrates that have been used for study of cell–matrix interactions [8]. These types of gels exhibit linear elastic responses up to approximately 100% strain [5]. Adherent cells on linear elastic substrates sense constant resistance to cell-generated forces either at early stages of adhesion formation when cells exert low forces, or later on in the cell adhesion process when forces exerted by cells increase [9]. By contrast, when cells adhere to nonlinear elastic substrates that exhibit strain stiffening, the cells may sense more environmental resistance at large substrate deformations [5]. In addition, as most strain-stiffening matrices are composed of rigid or semi-flexible polymers, large strains are also associated with alignment of filament and generation of spatially non-uniform deformations and stresses [10].

Collagen, the major structural protein of mammalian connective tissues [11], has been used extensively to model the structure and functions of many extracellular matrices and to assess how cells interact with matrix proteins in remodelling [12]. In naturally occurring biopolymers like collagen, many of the mechanical properties of the biopolymer are determined by physical constraints of the fibres in the network [13]. Accordingly, unlike elastic materials such as polyacrylamide hydrogels, the strain energy delivered by adherent cells to collagen gels is not completely stored in the network but instead can be dissipated because of the inelastic behaviour of the network. The amount of dissipated energy after application of cellular contractile forces may contribute to permanent deformation and the remodelling of fibres in the network [14]. The complex mechanics of naturally occurring biopolymers like collagen suggest that cells may not sense a constant resistance (elastic behaviour) or increasing resistance (strain-stiffening behaviour) when cell-generated contractile forces deform the network [5]. Accordingly, measurements of elastic properties at small strains and short times provide only limited information on the mechanical behaviour of naturally occurring biopolymers and the resultant compaction and remodelling of the network by cells.

The dual nature of elastic and inelastic behaviours of collagen matrices contributes to a strong dependency of their mechanical behaviour on loading conditions such as strain magnitude [5], loading history [15] and strain rate [16]. The amounts of dissipated energy and irreversible deformation may be influenced by the rate and magnitude of the strain. Consequently, biopolymers such as collagen or fibrin gels may exhibit distinct mechanical properties when subjected to, for example, relatively high rates of blood flow or low rates of applied forces by cells [15,16]. The mechanical behaviour of collagen matrices not only depends on the rigidity, diameter, length and concentration of individual collagen fibres in the network [17] and on the presence of intra and inter-fibrillar cross-links [18], but may also be influenced by external environmental factors such as the presence of an underlying rigid foundation or the proximity of boundary. Although elasticity theory [7] provides accurate predictions of the effect of an underlying rigid base on the mechanics of thin linearly elastic sheets, little is known about its influence on the mechanical behaviour of naturally occurring biopolymers like collagen gels. Because collagen gels are used extensively to examine cellular interactions with matrix proteins [19], we need to define their mechanical properties and the impact of external environmental factors for an improved understanding of mechanosensation.

We examined the mechanics of collagen matrices in the context of adherent cells that compact the pericellular collagen network at rates similar to that generated by adherent cells (in the order of micrometres per hour). With the use of rate-controlled compressive indentation of collagen gels, we found that the inelastic properties of collagen networks dominate their mechanical behaviour. We also discovered that the rigid foundations provided by glass or cell culture plastic to support collagen matrices impose additional mechanical constraints on the matrix, which reduce the inelastic behaviour of the network. We show that these features of cell culture models are important determinants of mechanosensation by adherent cells.

2. Material and methods

2.1. Model design and preparation of nylon meshes

Nylon mesh sheets with square openings (200 µm wide and individual fibre diameters of approx. 100 µm) were obtained from Dynamic Aqua-Supply (Surrey, British Columbia, Canada) and were used to provide support for collagen gels floated on cell culture medium. Fourteen single nylon fibres were removed vertically and horizontally to create grid opening sizes with defined geometries of 2×2 mm. This model design enabled measurements of cells located in the central region of the grid (electronic supplementary material, figure S1) where cells were not influenced by the presence of the nylon frames [20]. The model uses floating collagen matrices supported at their edges by nylon frames to uncouple matrix mechanics from an underlying solid foundation and removes possible mechanical constraints imposed by the foundation.

2.2. Preparation of floating and attached collagen samples

Collagen gels were prepared from pepsin-treated, bovine dermal type I collagen (6.0 mg ml^{-1}; approx. 97% type I collagen; Advanced BioMatrix, San Diego, CA, USA). Prior to experiments, collagen solutions were neutralized with 0.1 M NaOH to pH = 7.4 and diluted to a final concentration of 1 mg ml^{-1} or 3 mg ml^{-1} collagen. For preparation of floating gels, glass dishes were covered with stretched Parafilm to make a smooth, hydrophobic surface. Collagen solutions were poured on the prepared hydrophobic surface to produce collagen gels with thicknesses of 100 µm. The amount of collagen solution in each gel was adjusted depending on the area of each nylon mesh that was created. The nylon mesh was then placed on to the collagen, which filled the nylon grids with collagen solution. For preparation of attached gels, the coverglass to which gel must adhere firmly was activated. Briefly, coverglasses were immersed in 2% aminopropyltriethoxysilane (APTES; Sigma A36648; Oakville, Ontario, Canada) for 15 min at room temperature, followed by washing in acetone for 5 min and then air-dried for 15 min. Coverglasses were immersed in 0.1% w/w glutaraldehyde (GA, Sigma G5882) for 15 min on a shaker and rinsed three times (each time for 5 min) with autoclaved water. Appropriate volumes of collagen solutions were poured on to the prepared hydrophobic surface to produce collagen gels with thicknesses of 100 µm, which was verified by confocal microscopy optical sectioning. The nylon mesh was placed on to the collagen, which filled the nylon grids with collagen solution. Attached and floating samples were incubated at 37°C in 5% CO_2 until collagen polymerization was complete (90–120 min). For

preparation of floating gels, polymerized, collagen-coated nylon meshes were gently detached from the hydrophobic surface by addition of 1 × PBS and the floating collagen-coated meshes were inverted and immersed in cell-culture medium.

2.3. Cell culture

Fibroblasts (3T3 cells) were plated on attached or floating collagen gels supported by nylon mesh grids. Cells were plated in DMEM medium supplemented with 10% calf serum and 10% antibiotics. Cell plating densities were very low to enable the attachment of on average, only one to two cells in the central region of the grid. Cell culture was conducted at 37°C in a humidified 5% CO_2 environment for approximately 8 h.

2.4. Cell morphology and imaging

Cells were fixed in 4% paraformaldehyde and permeabilized with 0.2% Triton X-100. Cell morphology was visualized by rhodamine phalloidin (10^{-6} M) to stain actin filaments. Measurement of cell surface area was performed with ImageJ (v. 1.44) software. Cell extensions were measured from the cell centroid to the tip of the cell extension and were counted only if the length of extension was greater than 10 µm from the cell body. Cell nuclei were stained with DAPI. Focal adhesions were assessed by immunofluorescence staining for vinculin (Sigma) after cells were fixed with 4% paraformaldehyde. Fluorescent images were collected using 20× or 40× objectives with an inverted microscope (Nikon Eclipse).

2.5. Confocal microscopy

Collagen fibres were imaged using confocal reflectance microscopy with an inverted confocal laser scanning microscope (Leica TCS) using a 20 × dry or 40 × oil immersion objective lens (NA = 1.4). The thickness of the gel was measured from reconstructed *z*-stacks in the imaging mode (XYZ). For measurements of vinculin-immunostained focal adhesions, the total area of focal adhesions per cell was measured and then normalized for total cell area.

2.6. Analysis of local collagen fibre alignment

Fast Fourier transform (FFT) analysis was used to extract the orientation of collagen fibres from acquired images using confocal reflectance microscopy. FFT produces a spectrum image in the frequency domain of the original intensity image in the spatial domain [21]. Notably, the resulting image contains frequencies orthogonal to those in the original image. The FFT function of ImageJ (v. 1.44) software was used to generate the frequency content of the grey-scale images. In order to quantify the directionality of the original image, the pixel intensities in the resulting FFT image were summed along a straight line from the centre to the edge of the image at different angles. The summation process was performed using Oval Profile, an ImageJ plug-in (http://rsbweb.nih.gov/ij/plugins/oval-profile.html). The resulting plot was the sum of pixel intensities between 0° and 180°. A perfectly random image would result in an image with constant pixel intensity at different angles. By contrast, orientation of collagen fibres in a specific (non-random) direction would result in higher pixel intensities at a corresponding angle. A collagen fibre alignment index was estimated by calculation of the area under the intensity curve within ±10° of the peak.

2.7. Matrix deformation by cell-generated forces

Collagen solutions were mixed with fluorescent magnetite beads (2 µm diameter; Bangs Beads, Fishers, IN, USA), which served as fiduciary markers for tracking the deformation of the matrix under adherent cells. The relatively greater mass of magnetite beads compared with polystyrene beads enabled settling of the beads towards the bottom surface of the gel prior to polymerization. Gels were inverted after collagen polymerization was complete. The bead displacement field around each cell was mapped from a time series of phase contrast images that were collected using an inverted confocal laser scanning microscope with a 20 × air objective. The initial bead position was determined 90 min after cell seeding, when cells were attached to the gel surface. A time series of 70–90 images was collected at a frequency of one image every 5 min.

ImageJ software ('Align Slice' plug-in; https://weeman.inf.ethz.ch/ParticleTracker/) was used to align image stacks. Bead displacements and trajectories were estimated using the ImageJ plug-in, Particle Tracker (http://www.dentistry.bham.ac.uk/landinig/software/software.html). The maximum local fluorescence intensity was used as the estimate for the location of bead centres. The bead speed was measured from average of speed of all beads in the measurement field (i.e. 25–100 µm from the cell centroid). The depth of field of images in the *z*-axis was approximately 4 µm.

2.8. Mechanical characterization of collagen gels

A micro-indenter was used as described [22] to measure permanent deformation and maximum supported load exhibited by collagen gels. A cylindrical probe (25 µm in diameter with a flat probe tip), which is comparable to the diameters of spread cells, was used for indentation of collagen. Cyclic loading and unloading indentations were conducted on floating and attached collagen matrices supported by nylon grids. Collagen gels were indented in the middle of the grid with a 30 µm downward displacement and a 30 µm upward displacement at a speed of 15 µm s^{-1}, 1 µm s^{-1} and 1 µm min^{-1}, which is on the order of magnitude associated with cell-induced deformations of collagen matrices [23]. Loading/unloading indentation loops were analysed by calculating irreversible deformation (i.e. offset in the deformation axis) and maximum supported load (i.e. value of force at maximum indentation depth) [24].

2.9. Covalent cross-linking of collagen samples

To covalently cross-link the collagen samples, we treated polymerized collagen matrices with 0.5% GA (Sigma) in 1 × PBS for 2 h at room temperature. Samples were rinsed three times (15 min each) with PBS before performing experiments. We used propidium iodide (10 µg ml^{-1} final concentration; Sigma) to estimate cell viability approximately 8 h after initial cell attachment to cross-linked collagen matrices.

2.10. Measurement of water expulsion from collagen gels

We measured extrusion of water from collagen gels with a modification of a previously described method that employed ^3H_2O [25,26] and which we modified by substitution with a water-soluble fluorescent dye. Calcein (acetomethoxy ester; 50 µg, Invitrogen) was dissolved in 50 µl of DMSO and added to 1 ml of collagen solutions (1 mg ml^{-1} or 3 mg ml^{-1}). After collagen polymerization, 100 µl of water was quickly added on to the surface of gel samples and collected before application of cyclic indentation. After indentation of collagen samples, the same volume of water (100 µl) was added to the surface of collagen gels and then quickly collected. Photon counts attributable to calcein fluorescence in water samples and in collagen matrices were measured with a PTI fluorescence spectrophotometer (London, Ontario, Canada). The volume of extruded liquid was determined from the fluorescence intensity of calcein in the samples.

2.11. Statistical analysis

All continuous variables are reported as mean ± s.d. Pairwise comparisons for statistical significance were computed with unpaired Student's *t*-tests at a significance level of $p < 0.05$.

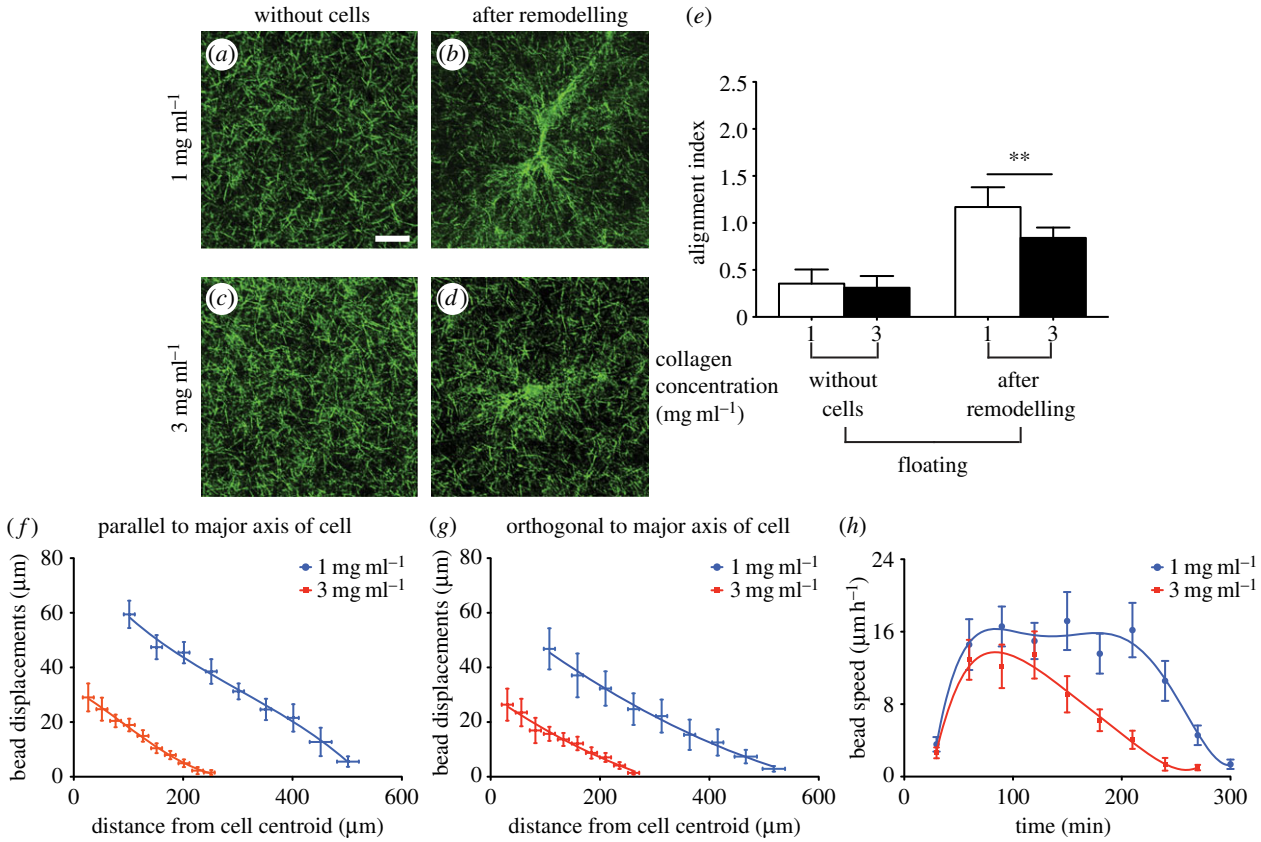

Figure 1. Cell-induced remodelling of thin floating gels. Collagen fibres in gels were aligned parallel to cell extensions after remodelling of the matrix by adherent cells. Collagen samples were imaged using confocal reflectance microscopy. Collagen fibres alignment and directionality were quantified using FFT analysis. Representative images of collagen fibres in gels of 1 mg ml^{-1} and 3 mg ml^{-1} collagen concentration before cell-induced remodelling (*a* and *c*) and after remodelling of the network by adherent cells (*b* and *d*), respectively. Pixel intensity in FFT analysis of at least 30 images of collagen fibres at the tip of cell extensions was summed along a straight line from the centre to the edge of the image at different angle provided information about collagen directionality and alignment. Alignment index was quantified by measurement of area under the intensity curve within $\pm 10^{\circ}$ of the peak (*e*). Propagation of cell-induced tension in collagen network was measured through displacement of embedded beads in the gel. Bead displacements were measured parallel (*f*) and orthogonal (*g*) to the longest cell extensions (i.e. major axis of the cell) in gels of 1 mg ml^{-1} and 3 mg ml^{-1} collagen concentration. The deformation rate (*h*) by adherent cells was measure through the average speed of beads in the cell periphery area (i.e. 25–100 μm from the cell centroid). Data are reported as mean $\pm$ s.d. $^{**}p < 0.01$ using unpaired Student's *t*-tests.

3. Results

3.1. Cell-induced reorganization of thin matrices without external environmental factors

Cell-generated tension in collagen matrices enables cells to sense the physical properties of their microenvironment and is evident from matrix reorganization and fibre alignment in the cell periphery. We employed thin floating collagen matrices to examine the effect of variation in collagen concentration in cell–matrix interactions and remodelling in the absence of physical boundaries. Visualization of collagen gels without cells showed that the distribution and orientation of collagen fibres across the gel width in floating collagen gels of 1 mg ml^{-1} or 3 mg ml^{-1} were similar (figure 1*a*,*c*). For gels without cells, FFT analysis showed no directional preference in fibre orientation in floating (electronic supplementary material, figure S2*a*,*c*) gels of different collagen concentrations. The low value of the alignment index (less than 0.4; figure 1*e*) for these collagen matrices indicated that the orientation of the collagen fibre network prior to cell attachment was random. After initial cell attachment to the gels, remodelling and reorganization of the collagen fibres occurred in less than 8 h (electronic supplementary material, figure S3). Reorganization of collagen fibres by adherent cells resulted in three to sixfold increases of the collagen fibre alignment index (electronic supplementary material, figure S2*b*,*d*). The estimates of alignment index for cells on floating collagen gels of 1 mg ml^{-1} (figure 1*b*) and 3 mg ml^{-1} (figure 1*d*) indicated that gels with a higher concentration of collagen undergo less remodelling by adherent cells than collagen gels with lower collagen concentration (approx. 40%; $p < 0.01$; figure 1*e*).

Alignment of collagen fibres along the direction of the load may facilitate propagation of cell-induced tension in the network. Accordingly, to examine how far cell tension is transmitted in networks of varying collagen concentrations, we measured bead displacement from the cell centroid. The measurement of bead displacements at positions along the longest cell extensions and perpendicular to the major axis of the cell indicated that in floating collagen gels (1 mg ml^{-1}), the bead displacements were greater (two to fourfold; $p < 0.0001$; figure 1*f*,*g*) than in 3 mg ml^{-1} collagen gels. The size of deformation fields was smaller in the floating gels of higher collagen concentration than the lower concentration gels ($p < 0.00001$). Furthermore, to assess the impact of collagen concentration on the dynamics of cell-mediated matrix deformation and reorganization, we measured the average speed of embedded marker beads in the cell periphery (i.e. 25–100 μm from the cell centroid). For both collagen concentrations, the compaction rate accelerated

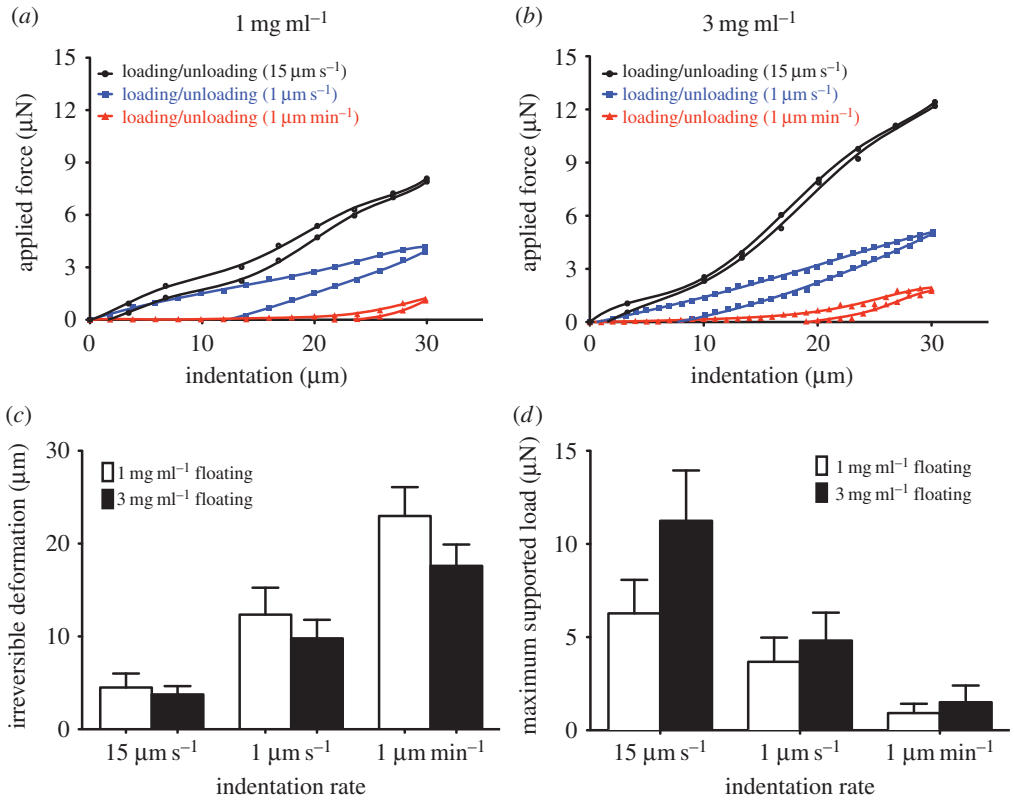

Figure 2. Measurement of elastic and inelastic mechanical behaviour of thin floating collagen gels. Cyclic indentation of floating gels of (*a*) 1 mg ml^{-1} and (*b*) 3 mg ml^{-1} collagen concentrations at indentation rates of 15 µm s^{-1}, 1 µm s^{-1} and 1 µm min^{-1}. A six-order polynomial was fitted to loading and unloading data. (*c*) The irreversible deformation was measured by calculation of the point where unloading function intersects *x*-axis. (*d*) The maximum supported force was measured from the value of loading function at maximum indentation depth (30 µm). Data are presented as mean ± s.d., minimum five measurements per each indentation rate per sample.

within 1–2 h after initial cell attachment and was in the range of 4–16 µm h^{-1} before decreasing to 0 µm per 30 min after 4 h. Cells on floating gels of 1 mg ml^{-1} collagen compacted collagen for 4–5 h after which there was no further compaction. By contrast, floating gels of 3 mg ml^{-1} collagen exhibited their maximal compaction rate at 90 min after initial attachment of the cells to the gel followed by a continuous decrease of compaction rate (figure 1*h*).

3.2. Cyclic strain loading of collagen gels

The dual nature of elastic and inelastic behaviours of collagen matrices may contribute to a combination of reversible and irreversible cell-mediated matrix remodelling. We employed cyclic loading and unloading indentation to examine the local mechanical properties of collagen networks, which provide estimates of the amount of reversible deformation (an indication of tension in the network) and irreversible cell-induced deformation of the network. These mechanical tests were conducted at varying deformation rates including a rate that is similar to that applied by adherent cells. Accordingly, we examined the mechanical behaviour of floating gels of 1 mg ml^{-1} and 3 mg ml^{-1} collagen concentrations by imposing compressive indentation at rates of 1 µm min^{-1}, 1 µm s^{-1} or 15 µm s^{-1}; we then quantified permanent deformations and maximum supported load of the collagen gels. The indentation depth (30 µm) was kept constant while continuous recordings were made of the resulting force at 0.5 s time intervals (figure 2*a*,*b*). The force-indentation cycles exhibited hysteresis on unloading, reflecting the dissipative loss of strain energy in the collagen network. All floating collagen samples at 1 mg ml^{-1} and 3 mg ml^{-1} exhibited some degree of hysteresis and irreversible compaction (figure 2*a*,*b*). However, the hysteresis behaviour, the amount of irreversible compaction and the supported load were strongly influenced by the rate of compressive indentation. Floating collagen gels subjected to slow indentation (1 µm min^{-1}) exhibited greater than fivefold ($p < 0.01$) larger irreversible deformation than fast indentation (15 µm s^{-1}). At slow indentation (1 µm min^{-1}), floating gels of 1 mg ml^{-1} exhibited approx. 30% more irreversible deformation than 3 mg ml^{-1} collagen gels (figure 2*c*; $p < 0.01$). By contrast, matrices of 1 mg ml^{-1} and 3 mg ml^{-1} subjected to fast indentation exhibited very similar amounts of irreversible deformation ($p > 0.8$). These data indicated that the force at maximum indentation (i.e. maximum supported load) exhibited by floating collagen matrices (1 mg ml^{-1} and 3 mg ml^{-1} collagen concentration) is proportional to the deformation rate. Dense collagen networks exhibited greater forces at maximum indentation than sparse networks when subjected to fast indentations ($p < 0.001$; figure 2*d*). By contrast, floating collagen gels (1 mg ml^{-1} and 3 mg ml^{-1} collagen concentration) subjected to slow deformations (1 µm min^{-1}) exhibited highly inelastic behaviour, which was manifest as very similar maximum supported load for dense and sparse networks ($p > 0.5$; figure 2*d*).

3.3. Effect of covalent cross-linking

To examine the influence of covalent cross-linking of collagen fibres on stress-relaxation and strain rate-dependent mechanics of collagen gels, we treated gels with 0.5% GA after the networks had fully polymerized [27,28]. When GA cross-linked collagen networks were subjected to cyclic loading and unloading, the rate-dependent inelastic behaviour was completely inhibited.

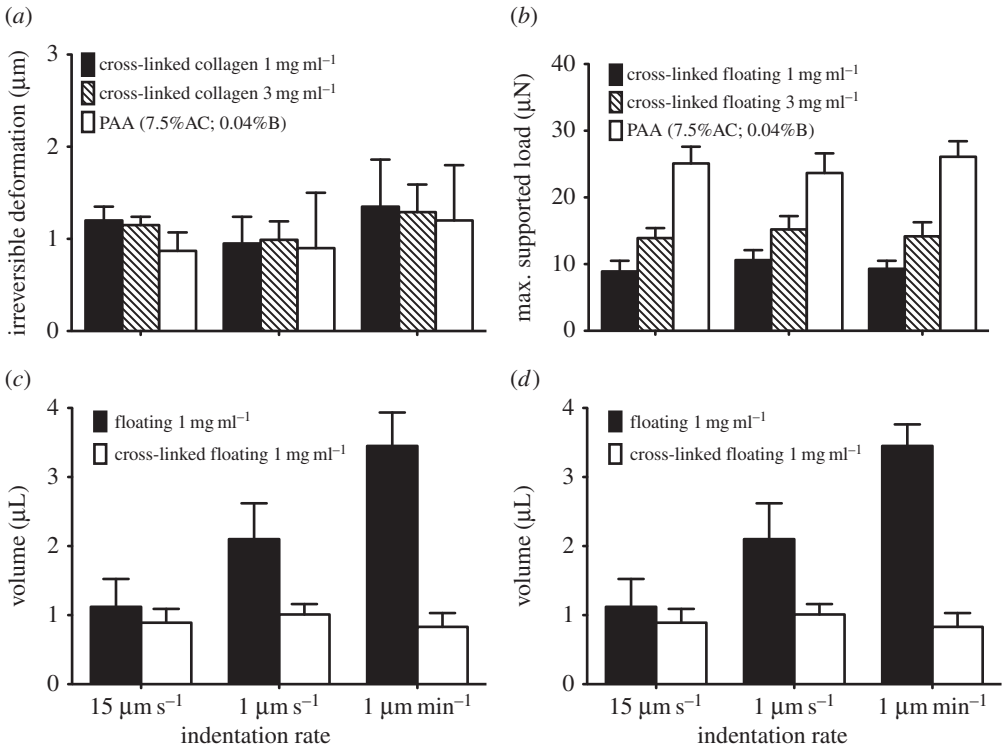

Figure 3. Effect of covalent cross-linking on the mechanical behaviour of thin floating gels and amount of water extruded from the collagen network. Thin collagen matrices were treated with 0.5% GA for 2 h prior to conducting mechanical tests. Polyacrylamide (PAA) hydrogels of 7.5% acrylamide and 0.04% of bis-acrylamide were used as control. The irreversible deformation (*a*) and maximum supported load (*b*) of cross-linked gels of 1 mg ml^{-1} and 3 mg ml^{-1} collagen concentration and PAA hydrogels are measured from cyclic loading/unloading indentations. The amount of water extruded from the cross-linked and non-cross-linked collagen samples of 1 mg ml^{-1} (*c*) and 3 mg ml^{-1} (*d*) collagen concentration was measured by incorporation of a water-soluble fluorescent dye (calcein) and photon counts attributable to calcein fluorescence in water samples (100 μl) and in collagen matrices. The volume of extruded liquid was determined from the fluorescence intensity of calcein in the samples. Data are presented as mean ± s.d., minimum three measurements per each indentation rate per sample.

All cross-linked collagen samples that were subjected to slow or fast indentations exhibited very low amounts of irreversible deformation (1–1.8 μm; figure 3*a*). Similarly, the maximum supported load was unchanged with decreasing strain rates from 15 μm s^{-1} to 1 μm min^{-1} (figure 3*b*; $p > 0.2$). Linearly elastic polyacrylamide hydrogels subjected to varying indentation rates exhibited a similar inelastic behaviour, which was manifested as less than 1 μm irreversible deformation and no change of maximum supported load (figure 3*a*,*b*; $p > 0.7$).

3.4. Water extrusion from collagen gels

When collagen gels are compressed, a pressure gradient and volume reduction will be induced in the gel; as a result, interfibrillar fluid will be extruded from the gel [26]. Accordingly, we measured the amount of extruded liquid from the gel-network, which may be associated with the inelastic behaviour of collagen fibres. The amount of extruded liquid from collagen gels was increased (greater than three-fold; $p < 0.0001$; figure 3*c*,*d*) with decreasing indentation speeds (from 15 μm s^{-1} to 1 μm min^{-1}). A smaller and rate-independent amount of liquid was extruded from GA cross-linked collagen gels (1 mg ml^{-1} and 3 mg ml^{-1} collagen concentration) that were subjected to varying indentation rates ($p > 0.1$; figure 3*c*,*d*).

3.5. Effect of an underlying rigid support

To examine the impact of external environmental factors such as an underlying rigid support on the mechanical behaviour of thin collagen networks, we assessed whether the amount of reversible and irreversible deformation after application of cyclic local indentation are influenced by the presence of physical boundaries. Accordingly, we quantified irreversible deformation and maximum supported load of thin, attached collagen gels subjected to varying deformation rates (1 μm min^{-1}, 1 μm s^{-1} or 15 μm s^{-1}). Similar to floating gels, attached gels exhibited some degrees of hysteresis (figure 4*a*,*b*). Similarly, the amount of irreversible deformation and maximum supported load exhibited by thin attached matrices was inversely proportional to the deformation rate and proportional to the deformation rate, respectively (figure 4*c*,*d*). However, attached gels subjected to slow deformations (1 μm s^{-1}) showed 30–50% less irreversible deformation compared with floating gels ($p < 0.001$). While attached gels of 3 mg ml^{-1} exhibited approximately 50% less irreversible deformation than gels of 1 mg ml^{-1} collagen concentration at fast indentations, both gels exhibited similar irreversible deformations at slow indentation (1 μm min^{-1}). Similarly, attached gels (1 mg ml^{-1} and 3 mg ml^{-1}) subjected to slow indentation exhibited very similar maximum supported load. By contrast, gels of 1 mg ml^{-1} showed approximately 40% less ($p < 0.01$) maximum supported load compared with 3 mg ml^{-1} gels at fast indentation rate (15 μm s^{-1}).

3.6. Effect of the presence of an underlying rigid support on cell–matrix interactions

The data described above indicated that the presence of underlying physical boundaries influenced the inelastic

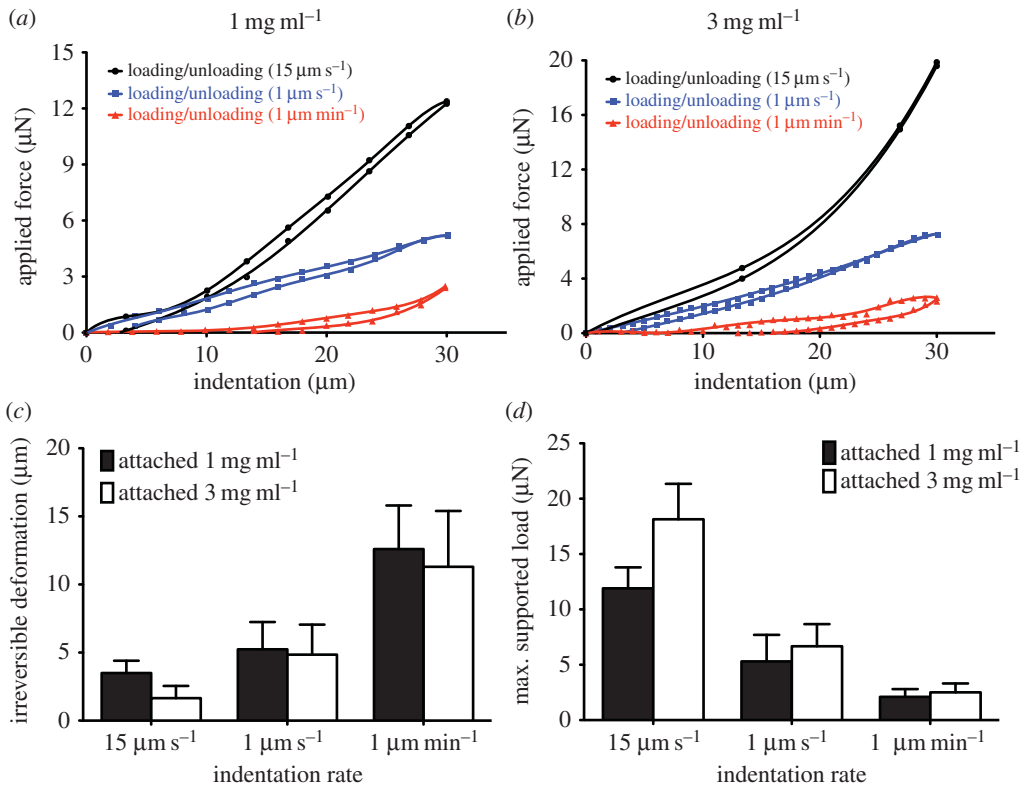

Figure 4. Effect of underlying rigid supports on the mechanical behaviour of thin collagen matrices. Collagen samples were prepared on activated coverglass so that the gel firmly adhered to the surface. Thin attached collagen gels of 1 mg ml^{-1} (*a*) and 3 mg ml^{-1} (*b*) collagen concentrations were imposed to cyclic loading and unloading mechanical tests at indentation rates of 15 µm s^{-1}, 1 µm s^{-1} and 1 µm min^{-1}. The irreversible deformation (*c*) and maximum supported load (*d*) were obtained from value of unloading function at 0 µN force and value of loading function at 30 µm indentation depth, respectively. Data are presented as mean ± s.d., minimum five measurements per each indentation rate per sample.

behaviour of thin collagen gels that are subjected to relatively slow deformation rates at rates that are similar to that applied by adherent cells. Accordingly, we examined how these alterations may impact cell-induced remodelling of collagen matrices. As the interactions between adherent cells and fibrillar collagen networks are strongly influenced by fibre geometry, physical properties [29] and network organization [30], we imaged collagen matrices prior to cell seeding and determined whether the presence of an underlying rigid foundation affects collagen fibre organization. Confocal reflected light microscopy was used to examine the effect of collagen concentration and the presence of an underlying rigid foundation on collagen gel organization [31,32]. Similar to floating gels, visualization of collagen gels without cells showed a similar distribution and orientation of collagen fibres across the gel width in both (1 mg ml^{-1} and 3 mg ml^{-1}) attached collagen gels (figure 5*a*,*c*). For gels without cells, FFT analysis showed no directional preference (electronic supplementary material, figure S4*a*,*d*) in fibre orientation in both attached gels of different collagen concentrations (figure 5*e*; $p > 0.06$). Collagen fibres were strongly aligned at the tips of cell extensions on attached gels (collagen concentration of 1 mg ml^{-1} or 3 mg ml^{-1}; figure 5*b*,*d*), which manifested as relatively high values of alignment index (approx. 2; figure 5*e*; electronic supplementary material, figure S4*b*,*d*) for these collagen matrices. Unlike floating gels, there was no significant difference in the alignment index ($p > 0.09$; figure 5*e*) between attached collagen gels of 1 mg ml^{-1} and 3 mg ml^{-1}. Furthermore, bead displacements and the size of deformation fields were similar in attached gels of 1 mg ml^{-1} and 3 mg ml^{-1} collagen concentration (figure 5*f*,*g*). Notably, attached gels (1 mg ml^{-1} and 3 mg ml^{-1}) exhibited smaller bead displacements (approx. 70–100%; $p < 0.001$) and smaller deformation fields (30–60%; $p < 0.001$) compared with floating gels. Cells on attached gels of 1 mg ml^{-1} or 3 mg ml^{-1} collagen showed similar trends in collagen compaction rate (figure 5*h*).

3.7. Effect of covalent cross-linking on cell–matrix interactions

As the cross-linking of collagen networks markedly reduced the inelastic behaviour of collagen matrices, we examined the impact of an underlying rigid foundation on interactions of cells with thin cross-linked collagen matrices. Viability assays using propidium iodide exclusion were used to assess the potential toxicity of the GA-treated collagen matrices. These data showed that 0.5% GA did not affect cell viability (electronic supplementary material, figure S5). In the absence of an underlying rigid foundation, FFT analysis showed no directional preference in fibre orientation in gels of collagen concentrations of 1 mg ml^{-1} (figure 6*a*) or 3 mg ml^{-1} (figure 6*b*), which manifested as a low alignment index for these collagen matrices (figure 6*e*).

Reorganization of collagen fibres by adherent cells after approximately 6 h from initial attachment to the gels resulted in approximately twofold increases of the collagen fibre alignment index in floating gels of collagen concentrations of 1 mg ml^{-1} (figure 6*c*; $p < 0.01$) and approximately 80% in gels of 3 mg ml^{-1} (figure 6*d*,*e*; $p < 0.05$). This analysis of network reorganization indicated that cross-linked gels with a lower concentration of collagen exhibited more

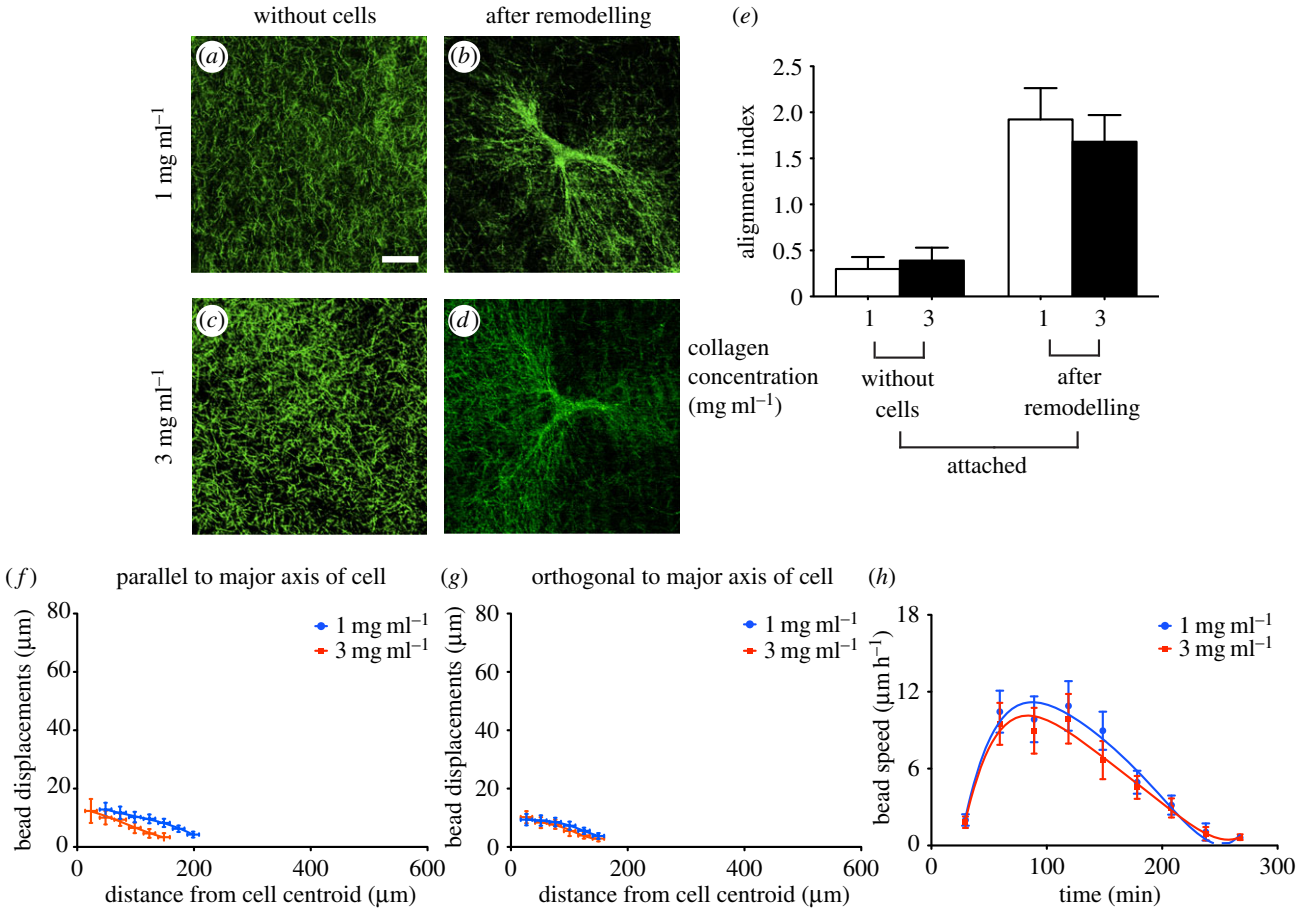

Figure 5. Cell–matrix interaction and the resultant matrix remodelling in the presence of underlying physical boundaries. Collagen fibres in attached gels of 1 mg ml^{-1} and 3 mg ml^{-1} collagen concentration were visualized with the use of confocal reflectance microscopy before (*a* and *c*, respectively) and after cell-induced remodelling of the network (*b* and *d*, respectively). FFT analysis was used to extract the orientation of collagen fibres from acquired images using confocal reflectance microscopy. Alignment index was quantified by measurement of area under the intensity curve within $\pm 10^{\circ}$ of the peak (*e*). Propagation of cell-induced tension in collagen network in the presence of an underlying rigid support was measured through displacement of embedded beads in the gel. Bead displacements were measured parallel (*f*) to the longest cell extensions and orthogonal to the major axis of the cell (*g*) in gels of 1 mg ml^{-1} and 3 mg ml^{-1} collagen concentration. The deformation rate (*h*) by adherent cells was measured through the average speed of beads in the cell periphery area (i.e. 25–100 μm from the cell centroid). Data are reported as mean ± s.d.

reorganization and remodelling by adherent cells than gels with a higher concentration of collagen (figure 6*e*; $p < 0.01$). Similarly, the average speed of embedded marker beads (an indication of the dynamics of cell–matrix deformation and remodelling) within 1–2 h from initial cell attachment was higher in gels of 1 mg ml^{-1} than 3 mg ml^{-1} collagen concentrations (figure 6*f*; $p < 0.05$).

Examination of attached collagen gels prior to cell attachment indicated that the presence of underlying physical boundaries did not affect collagen fibre organization and orientation (figure 6*g*,*h*). In the presence of an underlying rigid foundation, cells on cross-linked collagen gels of 1 mg ml^{-1} (figure 6*i*) and 3 mg ml (figure 6*j*) strongly aligned collagen fibres near the tips of cell extensions, which manifested as relatively high alignment indices (figure 6*k*). Similar to floating gels, there was more reorganization of collagen fibres in cells plated on lower collagen concentration gels than the higher collagen concentration (figure 6*k*; $p < 0.01$). Furthermore, the compaction rate, as estimated from the speed of marker beads in the cell periphery, indicated that the compaction rate after 1–2 h from cell attachment was higher in the lower collagen concentration gels (figure 6*l*; $p < 0.05$). Collectively, these data indicate that interactions of cell with cross-linked collagen matrices, which do not exhibit inelastic behaviour, were not influenced by the presence of underlying physical boundaries.

3.8. Cell mechanosensation

Resistance to cell-generated tension by the extracellular matrix can affect cell morphology and function [33]. Accordingly, we examined the influence of inelastic behaviours of thin collagen matrices on cell morphology. We cultured cells on the surface of attached (glass-supported) or floating collagen gels to assess mechanosensation in the presence or absence of a rigid foundation. Cells were well spread on attached collagen matrices (collagen concentrations of 1 mg ml^{-1} or 3 mg ml^{-1}; figure 7*a*,*b*), consistent with previous data [34,35]. By contrast, cells were less spread and exhibited sparse ($n < 4$), thin and relatively short cell extensions when cultured on floating gels (figure 7*c*,*d*). We quantified projected cell area (figure 7*e*) and the mean number of cell extensions per cell (figure 7*f*). Cells on collagen gels supported by a rigid foundation showed no difference of surface area when plated on 1 or 3 mg ml^{-1} collagen, whereas the surface area of cells on floating gels was approximately 40% greater ($p < 0.01$) on 3 mg ml gels than on 1 mg ml^{-1} gels. Collectively, these data indicate that

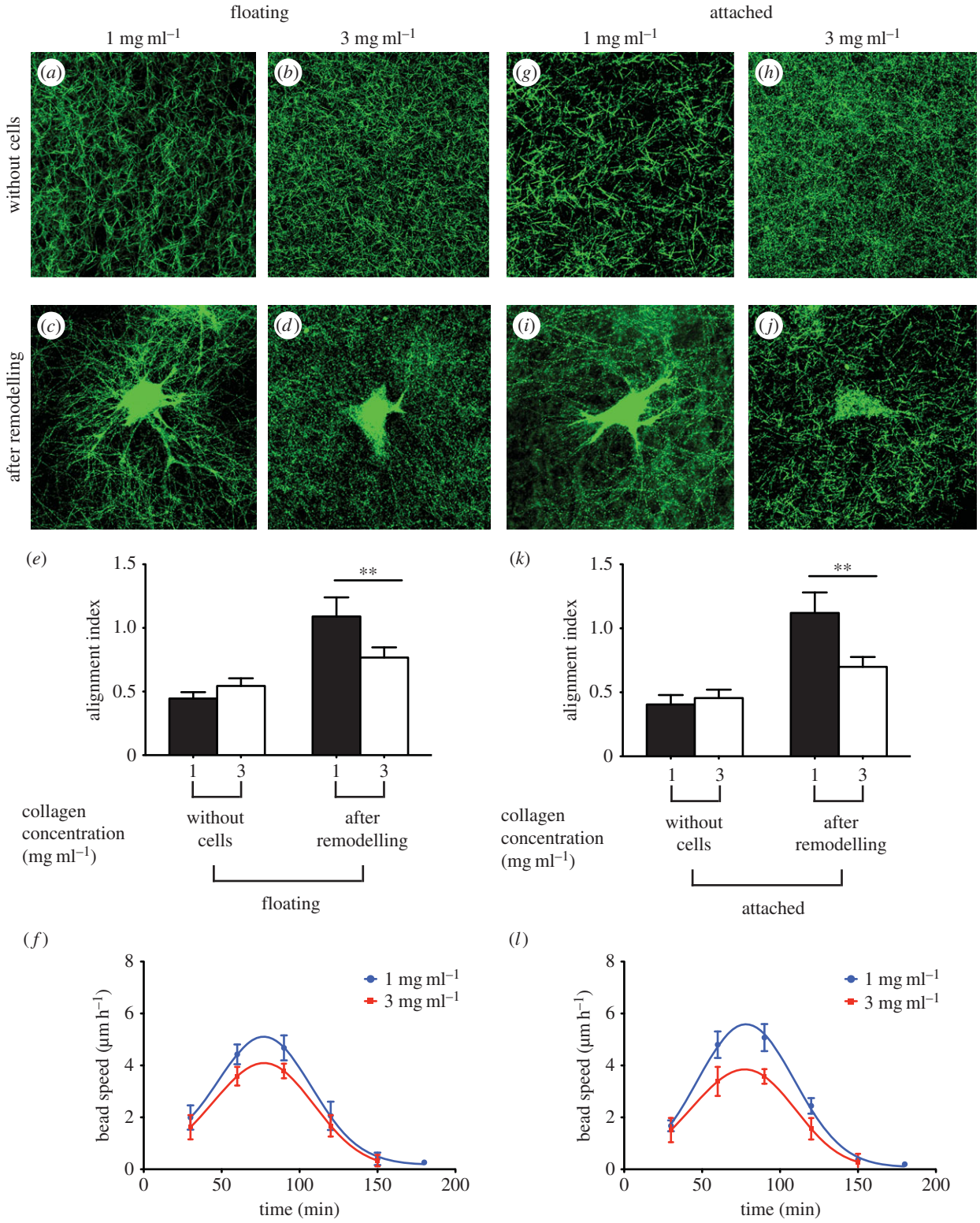

Figure 6. Cell-induced remodelling of cross-linked collagen matrices in the absence and presence of an underlying rigid foundation. Collagen matrices were treated with 0.5% GA prior to cell seeding. Collagen matrices of 1 mg ml^{-1} and 3 mg ml^{-1} collagen concentration were imaged using confocal reflectance microscopy. Representative images of collagen fibres in floating (*a–d*) and attached (*g–j*) cross-linked collagen networks before and after remodelling by adherent cells. Alignment index for floating (*e*) and attached (*k*) collagen matrices was quantified using FFT analysis of at least 30 images of collagen fibres at the tips of cell extensions. The deformation rate by adherent cell in cross-linked collagen matrices was measured from the average speed of beads in the cell periphery area for floating (*f*) and attached gels (*l*). Data are reported as mean ± s.d. $^{**}p < 0.01$ using unpaired Student's *t*-tests.

when supported by a rigid underlying foundation, cells on thin collagen matrices do not exhibit morphological responses to a higher collagen concentration (1 mg ml^{-1} compared with 3 mg ml^{-1}). However, cells on floating gels were more spread on 3 mg ml^{-1} gels compared with cells plated on 1 mg ml^{-1} collagen gels.

3.9. Cell mechanosensation on cross-linked collagen matrices

As cross-linked collagen networks did not exhibit inelastic behaviour, we examined the effect of an underlying foundation on the morphology of adherent cells on attached or

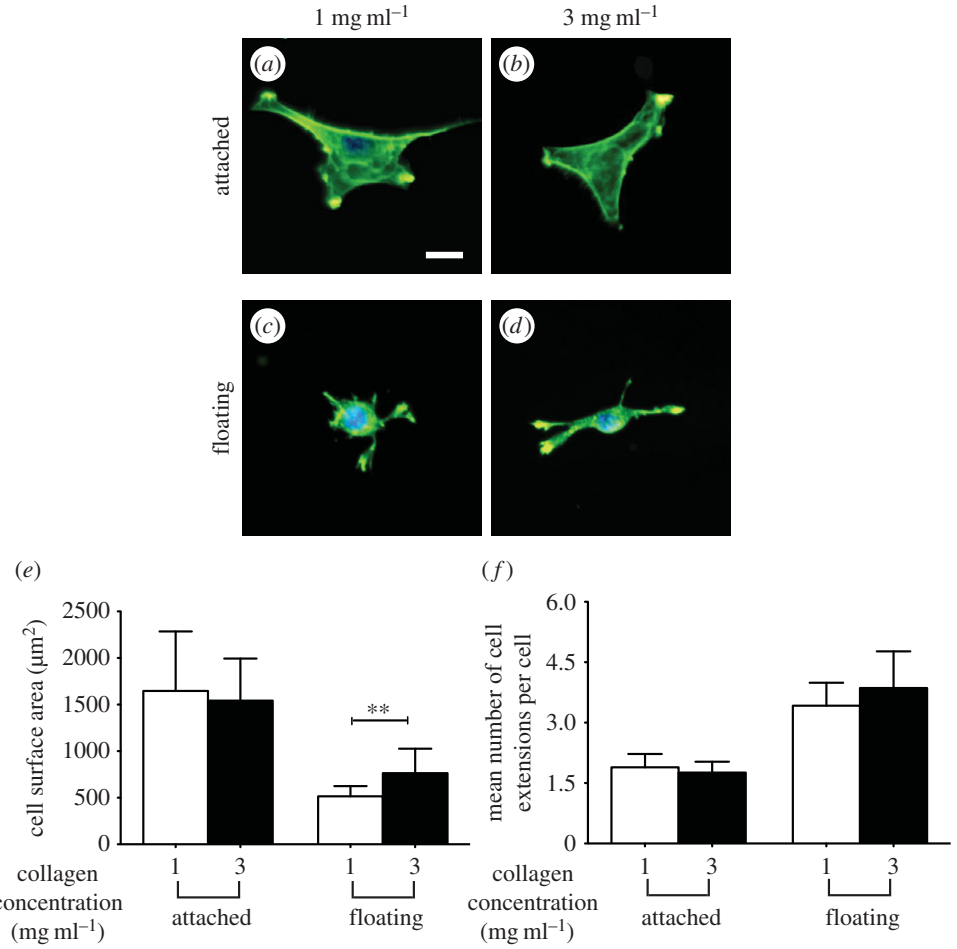

Figure 7. Cell surface area as an indicator of cellular mechanosensing on thin floating and attached collagen gels of varied concentrations. Representative fluorescent images of 3T3 fibroblast on thin attached and floating gels of 1 mg ml^{-1} (*a* and *c*, respectively) and 3 mg ml^{-1} (*b* and *d*, respectively) collagen concentration. Cell projected area (*e*) and the mean number of cell extensions/cell (*f*) as a function of physical properties (collagen concentration and out-of-plane physical boundary conditions). Data are reported as mean $\pm$ s.d. $^{**}p < 0.01$ using unpaired Student's *t*-tests. Scale bar, 20 μm. (Online version in colour.)

floating cross-linked gels. Unlike native (i.e. non-cross-linked) gels, cells adherent to cross-linked gels of 1 mg mg^{-1} (figure 8*a*,*b*) and 3 mg ml^{-1} collagen (figure 8*c*,*d*) did not exhibit morphological differences in the presence or absence of an underlying foundation. However, the projected surface area of cells was approximately 20% greater on gels of 3 mg ml^{-1} collagen concentration than on 1 mg ml^{-1} collagen (figure 8*e*; $p < 0.01$). Cells adherent to higher concentration collagen gels exhibited fewer cell extensions than lower concentration collagen gels (approx. fourfold; $p < 0.001$; figure 8*f*). These data indicate that cells do not respond to the presence of an underlying foundation on cross-linked collagen gels, which do not exhibit inelastic behaviour.

3.10. Focal adhesion formation in response to out-of-plane boundary conditions

In addition to cell spreading area, the size of focal adhesions is an indicator of cell mechanosensing [36,37]. We measured focal adhesion size to obtain insights into adhesion-dependent signalling processes [38,39]. Vinculin staining in the focal adhesions of cells adherent to attached or floating collagen gels of different concentration was quantified and normalized to total cell area. There was no significant deference in the normalized total area of focal adhesions in cells on attached collagen gels (1 mg ml^{-1} or 3 mg ml^{-1}; $p > 0.5$; figure 9*a*–*d*). By contrast, adherent cells on floating collagen gels of higher concentration (3 mg ml^{-1}; figure 9*g*,*h*) exhibited larger adhesions (approx. 30%; $p < 0.01$; figure 9*i*) than cells on lower concentration gels ($p < 0.01$; figure 9*e*,*f*).

4. Discussion

In this report, we used relatively wide, thin floating collagen matrices supported at their edges by nylon grids to study cell–matrix interactions unencumbered by external environmental factors such as the presence of lateral and underlying physical boundaries [20,34]. This model enables comparisons with cells on thin collagen matrices supported by an underlying rigid foundation without changing the thickness of the collagen. Variation of collagen thickness may markedly influence the network architecture and organization of collagen fibres in the network [40]. With this model, we found that the degree of collagen fibre alignment, the size of the nascent deformation field and the rate of network deformation by adherent cells was dependent on collagen concentration. Our data indicate that the alignment of fibres in the direction of the applied deformation was reduced in dense collagen networks compared with sparser networks, which in turn, may influence transmission of cell-induced mechanical signals through the network [41]. Indeed, our observations of bead displacement parallel with cell extensions demonstrate that cell-generated deformations are

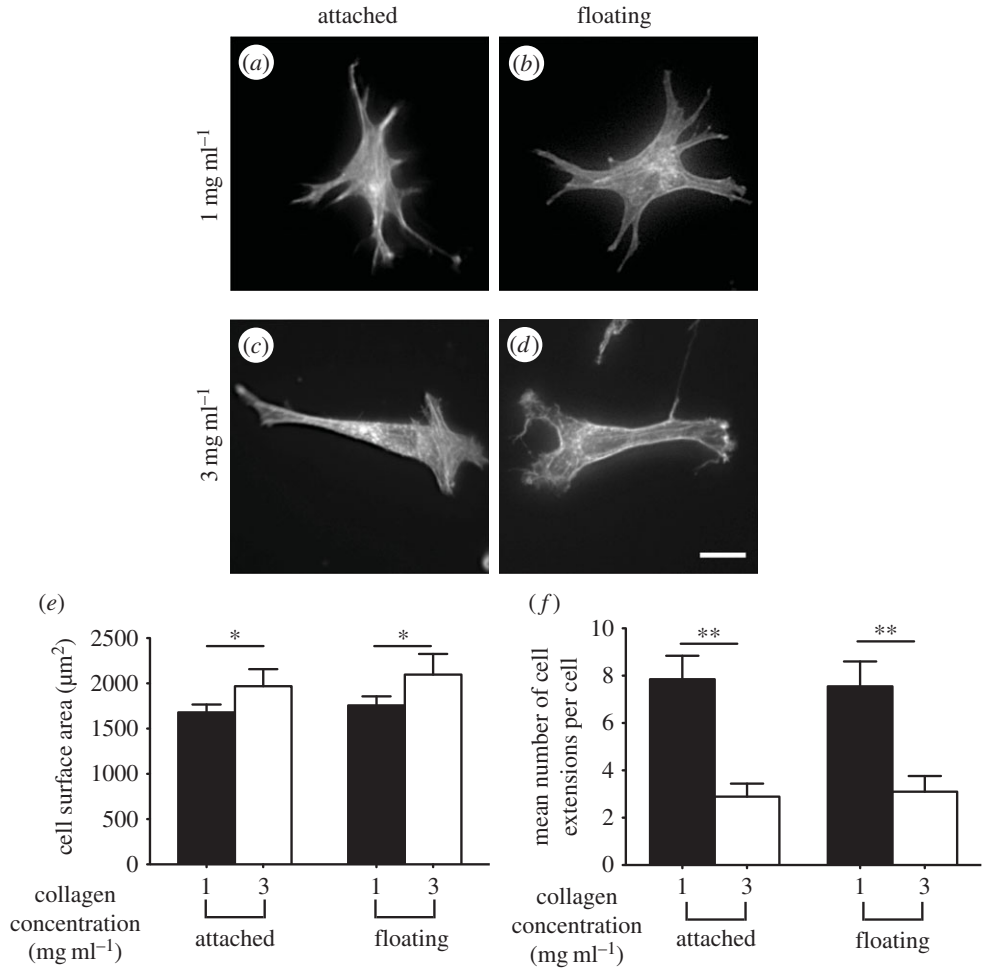

Figure 8. Morphology of cells adherent on cross-linked collagen matrices. Morphology of phalloidin-stained fibroblasts plated on attached and floating cross-linked collagen matrices of 1 mg ml^{-1} (*a*,*b*) and 3 mg ml^{-1} (*c*,*d*) collagen concentrations. Cell morphology was characterized by measurement of cell surface area (*e*) and mean number of cell extensions/cell (*f*). Data are mean $\pm$ s.d. from at least 40 cells. *$p < 0.01$, **$p < 0.001$ using unpaired Student's *t*-tests. Scale bar, 20 μm.

propagated further in sparse than in dense collagen networks. This collagen concentration-dependent effect on the transmission of mechanical signals may affect, for example, intercellular mechanical communication, which is fundamental to wound healing [42], tissue development [43] and cancer cell metastasis [44]. The collagen concentration-dependent remodelling of networks has been reported earlier [45], and it has been noted that the extent of network deformation decreases with higher collagen concentrations [46,47]. In contrast to these reports, our results show a much earlier decay in the rate of network deformation by adherent cells on dense networks. This finding may reflect higher levels of physical interactions because of the small pore size of the dense network [28].

Cell-induced deformation and remodelling of collagen networks are not wholly reversible because of the dual elastic and inelastic nature of collagen matrices [24]. The inelastic behaviour of collagen may arise from reorientation, slippage and extension of fibres in the network [15]. Notably, the irreversible inelastic properties of collagen preclude substantial resistance of the network to cell-induced deformation, which in turn may influence several cellular processes such as protease-independent migration of cancer cells [13]. Accordingly, examination of the elastic and inelastic behaviours of collagen networks at strain rates similar to cell-induced deformations may provide new insights into the extent of mechanical resistance to cell-induced matrix deformation and remodelling.

The mechanical behaviour of collagen matrices has been examined by shear, compression, tension and indentation methods, each with its own advantages and limitations [14]. The choice of methods depends on whether bulk or local properties of the matrix are of interest, which may be different because of the microstructure of collagen gels [23,48]. In this report, we used cyclic loading and unloading indentations, a well-defined method for measuring local mechanical properties of relatively thin soft tissues [49]. The anisotropic mechanics of collagen gels complicate measurements of the in-plane mechanical properties of collagen networks when deep, single micro-indentations are used [50]. However, analysis of cyclic loading/unloading indentation curves can be used to estimate the hysteresis, which is an indicator of the viscous properties of collagen networks [51], irreversible deformation (an indication of plastic deformation of the network; [24]) and the maximum supported load, which provides an indication of the degree of resistance to applied deformation and the amount of deformation energy stored in the network [52].

We found that the resistance of collagen matrices to deformation is dependent on the rate at which these networks are strained. This strain rate-dependent behaviour of thin collagen gels leads to a transition: from pronounced elastic behaviour at fast indentation to substantially inelastic behaviour at relatively slow indentation (similar rate as cell-mediated deformations). Our results demonstrate that collagen

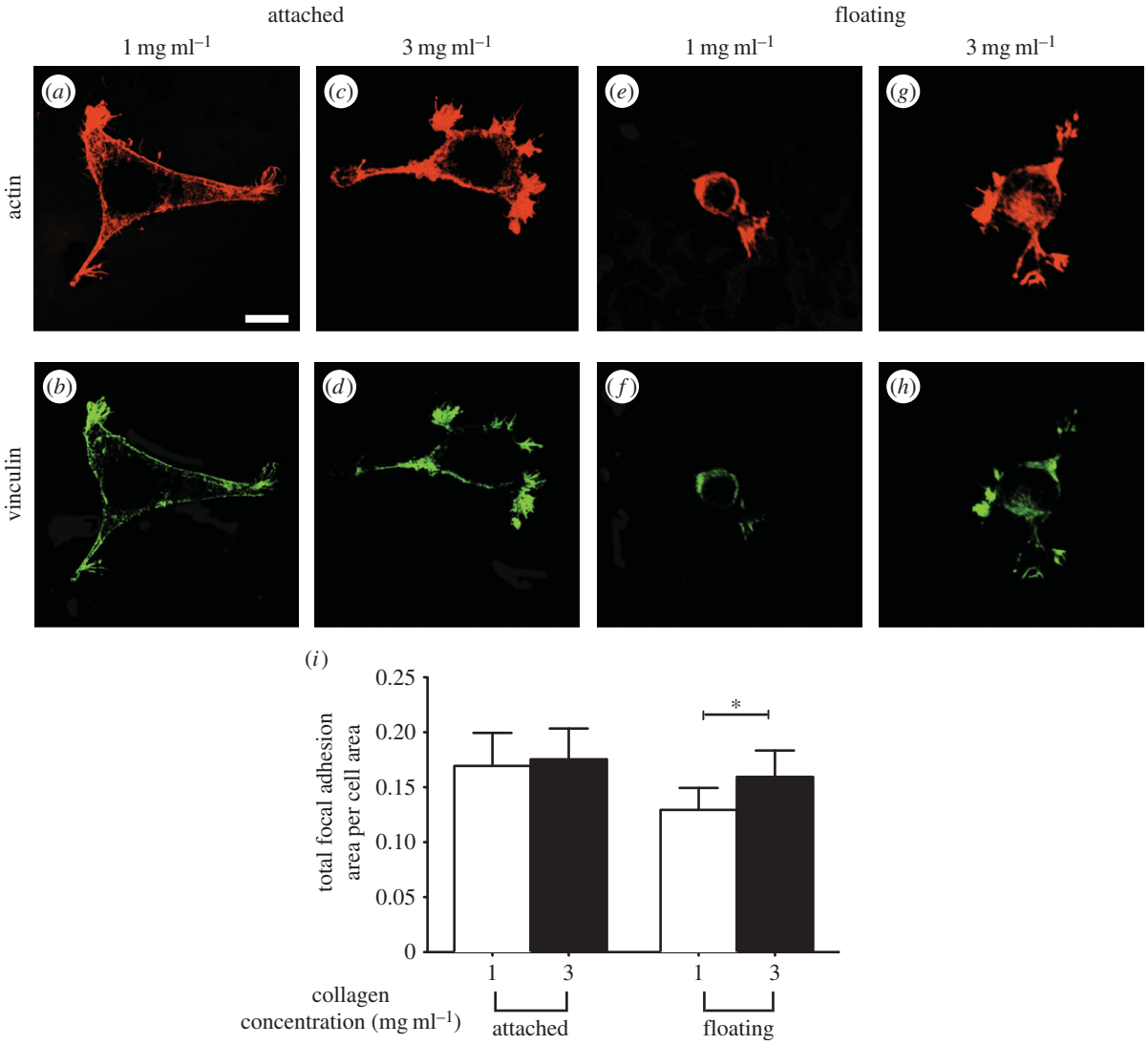

Figure 9. Impact of the presence of underlying physical boundaries on formation of focal adhesions. Adherent cells to collagen gels of indicated concentration, and physical boundary conditions were fixed and visualized by immunostaining for actin and vinculin. Actin filaments (phalloidin staining) and focal adhesions (vinculin staining) of cells on thin attached gels at collagen concentration of 1 mg ml^{-1} (*a* and *b*, respectively) and 3 mg ml^{-1} (*c* and *d*, respectively). Actin filaments (phalloidin staining) and focal adhesions (vinculin staining) of cells on thin floating gels at collagen concentration of 1 mg ml^{-1} (*e* and *f*, respectively) and 3 mg ml^{-1} (*g* and *h*, respectively). (*i*) Total focal adhesion area per cell as a function of physical properties and boundary conditions of their collagen matrices. Error bars represent s.d. At least 40 cells per group have been measured. Data shown are representative of three independent experiments. *p*-value was calculated with unpaired Student's *t*-tests (*$p < 0.01$). Scale bar, 20 µm. (Online version in colour.)

networks subjected to fast indentations exhibit larger resistance to deformation, which manifests as larger maximum supported force by the network. We attribute this mechanical property of collagen gels to limited reorganization of fibres in the network, possibly because of the relatively short relaxation time of collagen fibres and the minimal energy dissipation in the network [52]. This notion is consistent with previous studies on the elastic response of collagen networks subjected to relatively fast compressions [53]. With fast indentations, gels with higher collagen concentration exhibited less hysteresis and irreversible deformation, and larger supported force. These data are in agreement with our observation described above: as the collagen concentration is increased, the stiffer the network becomes and the network exhibits higher forces at given deformations [28]. By contrast, when collagen networks are subjected to slow deformations similar to those induced by cells, energy dissipation in the network is enhanced owing to the longer relaxation times, which enable reorganization of fibres and adaption of the network to the external deformations. This enhanced energy dissipation in the network is associated with reduced resistance to applied deformation, which results in more permanent deformation and reduced maximum supported force. Accordingly, cells that remodel and deform collagen networks may be in lower tension environments than cells that deform elastic synthetic substrates [54]. A substantial proportion of the tension on the collagen fibres is relaxed because of the marked inelastic behaviour of collagen networks at low deformation rates, which may be associated with the subsequent loss of stress fibres and fibronexus adhesion complexes of adherent cells [42]. This notion is consistent with previously reported results describing bulk elastic properties of collagen gels deformed at slow strain rates [16].

The inelastic behaviour of collagen gels is due in part to their high water content. The compaction of the collagen network results in reorganization of the gel and expulsion of unbound water, which reduces the gel volume. Previous work has shown that the volume of fibroblast-populated collagen matrices decreases because of the compaction of the network by the cells, which, in turn is associated with water

expulsion [25,26]. Thus, permanent deformation in the network may be associated with water loss in the network. Our results demonstrate that slow cyclic indentation of collagen gels causes more water extrusion from the network. We attribute this observation to the rearrangement and local compaction of collagen fibres around the tip of the microindenter, which increases the collagen density and reduces gel volume. Consistent with this notion, we found that GA cross-linked collagen gels did not exhibit strain rate-dependent extrusion of unbound water. We attribute this observation to the inhibition of slippage, lengthening and rearrangement of fibres in the network because of collagen cross-linking. Cross-linked collagen fibres do not relax their internal tension, thereby resisting applied deformation, which manifests as strain rate-independent mechanical behaviour. Consistent with our results, several studies have reported similar mechanical behaviour of collagen networks after cross-linking [30]. Glutaraldehyde-treated collagen networks support higher tension in the network [27]. The fibre alignment and network density in the cross-linked network are reversible effects, indicating that the enhanced inelastic behaviour of the collagen network is primarily because of non-permanent coupling of collagen fibres in the network [15,30].

We found that cells on floating collagen gels responded to variations in collagen concentration by displaying greater surface area, as previously reported [55], whereas cells on thin attached gels of different collagen concentration were equally well spread. We suggest that this difference may be because thin attached gels of different concentrations (1 mg ml^{-1} or 3 mg ml^{-1}) exhibited nearly the same inelastic behaviour, which is affected more by the presence of an underlying support than the concentration of collagen fibres. By contrast, floating gels of higher collagen concentration exhibited less inelastic behaviour, which was manifest as lower hysteresis and permanent deformations. These data are in agreement with our findings of reduced local remodelling of collagen fibres in dense networks. Our observations are also consistent with the previously reported surface area of 3T3 fibroblast cells on thin gels at collagen concentration of 4 mg ml^{-1} [35]: although the collagen concentration was increased fourfold, cell surface area was not significantly increased. We also found that collagen fibres were more aligned at the tips of cell extensions in thin attached gels than floating gels. While this enhanced local alignment of collagen fibres may arise from higher applied forces by adherent cells, the resultant forces did not evidently expand the deformation fields. We attribute this observation to the influence of an underlying rigid foundation on the mechanics of thin collagen matrices, which exhibited less inelastic behaviour. Accordingly, cell-generated stresses and strains may not be completely propagated through collagen networks that are supported by an underlying rigid foundation. This notion is also supported by the smaller bead displacements at each point along the cell extensions in thin attached gels compared with floating gels.

Remote, in-depth mechanosensing is thought to influence the morphology and function of cells plated on thin attached matrices [41,42], but this notion needs to consider the effect of rigid foundations on the mechanics of collagen gels. Unlike elastic substrates that preserve cell-induced tension in the network, native collagen matrices also exhibit inelastic behaviour, which can release cell-generated tension. Because the maintenance and resistance of cell-induced tension by the matrix affects cell morphology and function [33], the inelastic behaviour of the matrix likely impacts cell morphology and function. Indeed, our data indicate that thin matrices supported by an underlying rigid support exhibit less inelastic behaviour and maintain higher levels of tension in the network. These findings are consistent with earlier data showing that cell surface area and formation of focal adhesions are affected by the presence of underlying physical boundaries, similar to cells in high tension environments [42]. Notably, we show that the mechanical behaviour of cross-linked matrices, which do not exhibit inelastic behaviour, was not affected by the presence of physical boundaries. Similarly, adherent cells on cross-linked collagen matrices did not respond to the presence or absence of the underlying rigid foundation.

5. Conclusion

We examined the impact of the inelastic behaviour of collagen gels on cell–matrix interactions. We conclude that cell-induced remodelling and mechanosensation are strongly influenced by the inelastic behaviour of collagen matrices, particularly at strain rates generated by cells. Constrained, thin matrices exhibit less inelastic behaviour and are able to maintain higher level of tension, which in turn affect cell–matrix interactions and mechanosensation by adherent cells.

Funding statement. H.M. gratefully acknowledges financial support from a CIHR Strategic Training fellow, STP-53877. The research was supported by CIHR operating grant to C.A.M. (MOP-490422), who is also supported by a Canada Research Chair (Tier 1).

References

1. Mierke CT. 2014 The fundamental role of mechanical properties in the progression of cancer disease and inflammation. *Rep. Prog. Phys.* **77**, 076602. (doi:10.1088/0034-4885/77/7/076602)
2. Wang N, Butler JP, Ingber DE. 1993 Mechanotransduction across the cell surface and through the cytoskeleton. *Science* **260**, 1124–1127. (doi:10.1126/science.7684161)
3. Choquet D, Felsenfeld DP, Sheetz MP. 1997 Extracellular matrix rigidity causes strengthening of integrin–cytoskeleton linkages. *Cell* **88**, 39–48. (doi:10.1016/S0092-8674(00)81856-5)
4. Janmey PA, Schliwa M. 2008 Rheology. *Curr. Biol.* **18**, R639–R641. (doi:10.1016/j.cub.2008.05.001)
5. Storm C, Pastore JJ, MacKintosh FC, Lubensky TC, Janmey PA. 2005 Nonlinear elasticity in biological gels. *Nature* **435**, 191–194. (doi:10.1038/nature03521)
6. Timoshenko SP, Gere JM. 2012 *Theory of elastic stability*. New York, NY: Courier Dover Publications.
7. Landau LD, Lifshitz EM. 1987 *Theory of elasticity*, 2nd edn, vol. 7. New York, NY: Pergamon.
8. Pelham Jr RJ, Wang Y. 1997 Cell locomotion and focal adhesions are regulated by substrate flexibility. *Proc. Natl Acad. Sci. USA* **94**, 13 661–13 665. (doi:10.1073/pnas.94.25.13661)
9. Rape AD, Guo WH, Wang YL. 2011 The regulation of traction force in relation to cell shape and focal adhesions. *Biomaterials* **32**, 2043–2051. (doi:10.1016/j.biomaterials.2010.11.044)
10. Wen Q, Basu A, Janmey PA, Yodh AG. 2012 Non-affine deformations in polymer hydrogels. *Soft Matter* **8**, 8039–8049. (doi:10.1039/c2sm25364j)
11. Gross J, Highberger JH, Schmitt FO. 1952 Some factors involved in the fibrogenesis of collagen

in vitro. *Proc. Soc. Exp. Biol. Med.* **80**, 462–465. (doi:10.3181/00379727-80-19657)

12. Grinnell F, Petroll WM. 2010 Cell motility and mechanics in three-dimensional collagen matrices. *Annu. Rev. Cell Dev. Biol.* **26**, 335–361. (doi:10.1146/annurev.cellbio.042308.113318)
13. Mohammadi H, McCulloch CA. 2013 Impact of elastic and inelastic substrate behaviors on mechanosensation. *Soft Matter* **10**, 408–420. (doi:10.1039/c3sm52729h)
14. Billiar KL. 2011 The mechanical environment of cells in collagen gel models. In *Cellular and biomolecular mechanics and mechanobiology* (ed. A Gefen), pp. 201–245. Berlin, Germany: Springer. (doi:10.1007/8415_2010_30)
15. Munster S, Jawerth LM, Leslie BA, Weitz JI, Fabry B, Weitz DA. 2013 Strain history dependence of the nonlinear stress response of fibrin and collagen networks. *Proc. Natl Acad. Sci. USA* **110**, 12 197–12 202. (doi:10.1073/pnas.1222787110)
16. Lopez-Garcia MD, Beebe DJ, Crone WC. 2010 Young's modulus of collagen at slow displacement rates. *Biomed. Mater. Eng.* **20**, 361–369. (doi:10.3233/BME-2010-0649)
17. Yang YL, Kaufman LJ. 2009 Rheology and confocal reflectance microscopy as probes of mechanical properties and structure during collagen and collagen/hyaluronan self-assembly. *Biophys. J.* **96**, 1566–1585. (doi:10.1016/j.bpj.2008.10.063)
18. Motte S, Kaufman LJ. 2013 Strain stiffening in collagen I networks. *Biopolymers* **99**, 35–46. (doi:10.1002/bip.22133)
19. Grinnell F. 2003 Fibroblast biology in three-dimensional collagen matrices. *Trends Cell Biol.* **13**, 264–269. (doi:10.1016/S0962-8924(03)00057-6)
20. Mohammadi H, Janmey PA, McCulloch CA. 2014 Lateral boundary mechanosensing by adherent cells in a collagen gel system. *Biomaterials* **35**, 1138–1149. (doi:10.1016/j.biomaterials.2013.10.059)
21. Ballard DH. 1981 Generalizing the Hough transform to detect arbitrary shapes. *Pattern Recognit.* **13**, 111–122. (doi:10.1016/0031-3203(81)90009-1)
22. Levental I, Levental KR, Klein EA, Assoian R, Miller RT, Wells RG, Janmey PA. 2010 A simple indentation device for measuring micrometer-scale tissue stiffness. *J. Phys. Condens. Matter* **22**, 194120. (doi:10.1088/0953-8984/22/19/194120)
23. Pizzo AM, Kokini K, Vaughn LC, Waisner BZ, Voytik-Harbin SL. 2005 Extracellular matrix (ECM) microstructural composition regulates local cell-ECM biomechanics and fundamental fibroblast behavior: a multidimensional perspective. *J. Appl. Physiol.* **98**, 1909–1921. (doi:10.1152/japplphysiol.01137.2004)
24. Fung YC. 1993 *Biomechanics: mechanical properties of living tissues*, 2nd edn. New York, NY: Springer.
25. Arora PD, Narani N, McCulloch CA. 1999 The compliance of collagen gels regulates transforming growth factor-beta induction of alpha-smooth muscle actin in fibroblasts. *Am. J. Pathol.* **154**, 871–882. (doi:10.1016/S0002-9440(10)65334-5)
26. Nakagawa S, Pawelek P, Grinnell F. 1989 Long-term culture of fibroblasts in contracted collagen gels: effects on cell growth and biosynthetic activity. *J. Invest. Dermatol.* **93**, 792–798. (doi:10.1111/1523-1747.ep12284425)
27. Chandran PL, Paik DC, Holmes JW. 2012 Structural mechanism for alteration of collagen gel mechanics by glutaraldehyde crosslinking. *Connect. Tissue Res.* **53**, 285–297. (doi:10.3109/03008207.2011.640760)
28. Miron-Mendoza M, Seemann J, Grinnell F. 2010 The differential regulation of cell motile activity through matrix stiffness and porosity in three dimensional collagen matrices. *Biomaterials* **31**, 6425–6435. (doi:10.1016/j.biomaterials.2010.04.064)
29. Ito Y. 1999 Surface micropatterning to regulate cell functions. *Biomaterials* **20**, 2333–2342. (doi:10.1016/S0142-9612(99)00162-3)
30. Vader D, Kabla A, Weitz D, Mahadevan L. 2009 Strain-induced alignment in collagen gels. *PLoS ONE* **4**, e5902. (doi:10.1371/journal.pone.0005902)
31. Boyde A, Wolfe LA, Maly M, Jones SJ. 1995 Vital confocal microscopy in bone. *Scanning* **17**, 72–85. (doi:10.1002/sca.4950170203)
32. Friedl P. 2004 Dynamic imaging of cellular interactions with extracellular matrix. *Histochem. Cell Biol.* **122**, 183–190. (doi:10.1007/s00418-004-0682-0)
33. Ingber DE. 2003 Mechanosensation through integrins: cells act locally but think globally. *Proc. Natl Acad. Sci. USA* **100**, 1472–1474. (doi:10.1073/pnas.0530201100)
34. Leong WS, Tay CY, Yu H, Li A, Wu SC, Duc DH, Lim CT, Tan LP. 2010 Thickness sensing of hMSCs on collagen gel directs stem cell fate. *Biochem. Biophys. Res. Commun.* **401**, 287–292. (doi:10.1016/j.bbrc.2010.09.052)
35. Rudnicki MS, Cirka HA, Aghvami M, Sander EA, Wen Q, Billiar KL. 2013 Nonlinear strain stiffening is not sufficient to explain how far cells can feel on fibrous protein gels. *Biophys. J.* **105**, 11–20. (doi:10.1016/j.bpj.2013.05.032)
36. Hoffman BD, Grashoff C, Schwartz MA. 2011 Dynamic molecular processes mediate cellular mechanotransduction. *Nature* **475**, 316–323. (doi:10.1038/nature10316)
37. Prager-Khoutorsky M, Lichtenstein A, Krishnan R, Rajendran K, Mayo A, Kam Z, Geiger B, Bershadsky AD. 2011 Fibroblast polarization is a matrix-rigidity-dependent process controlled by focal adhesion mechanosensing. *Nat. Cell Biol.* **13**, 1457–1465. (doi:10.1038/ncb2370)
38. Rajshankar D, Downey GP, McCulloch CA. 2012 IL-1beta enhances cell adhesion to degraded fibronectin. *FASEB J.* **26**, 4429–4444. (doi:10.1096/fj.12-207381)
39. Wang Q, Downey GP, McCulloch CA. 2011 Focal adhesions and Ras are functionally and spatially integrated to mediate IL-1 activation of ERK. *FASEB J.* **25**, 3448–3464. (doi:10.1096/fj.11-183459)
40. Carey SP, Kraning-Rush CM, Williams RM, Reinhart-King CA. 2012 Biophysical control of invasive tumor cell behavior by extracellular matrix microarchitecture. *Biomaterials* **33**, 4157–4165. (doi:10.1016/j.biomaterials.2012.02.029)
41. Ma X, Schickel ME, Stevenson MD, Sarang-Sieminski AL, Gooch KJ, Ghadiali SN, Hart RT. 2013 Fibers in the extracellular matrix enable long-range stress transmission between cells. *Biophys. J.* **104**, 1410–1418. (doi:10.1016/j.bpj.2013.02.017)
42. Tomasek JJ, Gabbiani G, Hinz B, Chaponnier C, Brown RA. 2002 Myofibroblasts and mechano-regulation of connective tissue remodelling. *Nat. Rev.* **3**, 349–363. (doi:10.1038/nrm809)
43. Daley GQ. 2008 Common themes of dedifferentiation in somatic cell reprogramming and cancer. *Cold Spring Harb. Symp. Quant. Biol.* **73**, 171–174. (doi:10.1101/sqb.2008.73.041)
44. Friedl P, Sahai E, Weiss S, Yamada KM. 2012 New dimensions in cell migration. *Nat. Rev. Mol. Cell Biol.* **13**, 743–747. (doi:10.1038/nrm3459)
45. Helary C, Bataille I, Abed A, Illoul C, Anglo A, Louedec L, Letourneur D, Meddahi-Pelle A, Giraud-Guille MM. 2010 Concentrated collagen hydrogels as dermal substitutes. *Biomaterials* **31**, 481–490. (doi:10.1016/j.biomaterials.2009.09.073)
46. Kwok CB, Ho FC, Li CW, Ngan AH, Chan D, Chan BP. 2013 Compression-induced alignment and elongation of human mesenchymal stem cell (hMSC) in 3D collagen constructs is collagen concentration dependent. *J. Biomed. Mater. Res. A* **101**, 1716–1725. (doi:10.1002/jbm.a.34475)
47. Nishiyama T, Tominaga N, Nakajima K, Hayashi T. 1988 Quantitative evaluation of the factors affecting the process of fibroblast-mediated collagen gel contraction by separating the process into three phases. *Collagen Relat. Res.* **8**, 259–273. (doi:10.1016/S0174-173X(88)80045-1)
48. Roeder BA, Kokini K, Voytik-Harbin SL. 2009 Fibril microstructure affects strain transmission within collagen extracellular matrices. *J. Biomech. Eng.* **131**, 031004. (doi:10.1115/1.3005331)
49. Reilly GC, Engler AJ. 2010 Intrinsic extracellular matrix properties regulate stem cell differentiation. *J. Biomech.* **43**, 55–62. (doi:10.1016/j.jbiomech.2009.09.009)
50. Cox MA, Driessen NJ, Boerboom RA, Bouten CV, Baaijens FP. 2008 Mechanical characterization of anisotropic planar biological soft tissues using finite indentation: experimental feasibility. *J. Biomech.* **41**, 422–429. (doi:10.1016/j.jbiomech.2007.08.006)
51. Achilli M, Meghezi S, Mantovani D. 2012 On the viscoelastic properties of collagen-gel-based lattices under cyclic loading: applications for vascular tissue engineering. *Macromol. Mater. Eng.* **297**, 724–734. (doi:10.1002/mame.201100363)
52. Silver FH. 2006 *Mechanosensing and mechanochemical transduction in extracellular matrix*. Berlin, Germany: Springer.
53. Chandran PL, Barocas VH. 2004 Microstructural mechanics of collagen gels in confined compression: poroelasticity, viscoelasticity, and collapse. *J. Biomech. Eng.***126**, 152–166. (doi:10.1115/1.1688774)
54. Discher DE, Janmey P, Wang YL. 2005 Tissue cells feel and respond to the stiffness of their substrate. *Science* **310**, 1139–1143. (doi:10.1126/science.1116995)
55. Engler A, Bacakova L, Newman C, Hategan A, Griffin M, Discher D. 2004 Substrate compliance versus ligand density in cell on gel responses. *Biophys. J.* **86**, 617–628. (doi:10.1016/S0006-3495(04) 74140-5)